https://doi.org/10.5194/egusphere-2024-2797
Preprint. Discussion started: 19 September 2024
© Author(s) 2024. CC BY 4.0 License.

Analyzing the chemical composition, morphology and size of ice-nucleating particles by coupling a scanning electron microscope to an offline diffusion chamber

Lisa Schneider[1], Jann Schrod[2], Daniel Weber[2,a], Heinz Bingemer[2], Konrad Kandler[1], Joachim Curtius[2], Martin Ebert[1]

[1]Institute of Applied Geoscience, Technical University of Darmstadt, Darmstadt, 64287, Germany
[2]Institute for Atmospheric and Environmental Sciences, Goethe University Frankfurt, Frankfurt am Main, 60438, Germany
[a]now at: Federal Waterways Engineering and Research Institute, Karlsruhe, 76187, Germany

Correspondence to: Lisa Schneider (schneider@geo.tu-darmstadt.de); Martin Ebert (mebert@geo.tu-darmstadt.de)

Abstract. To understand and predict the formation of clouds and rain and their influence on our climate, it is crucial to know the characteristics and abundance of ice-nucleating particles (INPs) in the atmosphere. As the ice-nucleating efficiency is a result of individual particle properties, a detailed knowledge on these properties is essential. Here, we present an offline method for the comprehensive analysis of ambient INPs that benefits from the combination of two instruments already used for ice nucleation measurements. First, the aerosol is sampled on silicon wafers. INPs are then activated at different temperature and humidity conditions in the deposition nucleation and condensation freezing mode using a static diffusion chamber. Activated INPs are located in a coordinate system, which allows for recovery of the individual particles causing the nucleation in a scanning electron microscope. Here, the size, chemistry and morphology of the particles are identified. Finally, the INPs are classified into categories based on their measured properties. As a result, a size resolved spectrum of the INP classes can be determined.

The performance of this coupling method is investigated in a case study on samples from the high-altitude field side Jungfraujoch (JFJ), Switzerland. 200 individual INPs from 14 samples obtained during a 5-week period were classified. Most deposition nucleation / condensation freezing mode INPs from Jungfraujoch, activated at -30 °C, were of irregular shape and had projected area diameters in the range from 300 nm to 35 µm, with a distinct maximum at 1 - 2 µm. A major contribution of mineral particles, mainly aluminosilicates / Al-rich particles, but also carbonates and silica, was identified for the entire INP size spectrum at -30°C. Further contributions were from carbon-rich particles, consisting of both smaller soot particles and larger biological particles. Mixed particles, here mostly particles rich in Al and C, were identified in higher abundances primarily between 3 µm and 9 µm. Minor contributions were seen from sulfates and metal oxides, with the latter ones found with increased proportion in the size range below 500 nm.

Such results are useful for evaluating INP type-specific parametrizations, e.g., for use in atmospheric modeling, and in closure studies.

https://doi.org/10.5194/egusphere-2024-2797
Preprint. Discussion started: 19 September 2024
© Author(s) 2024. CC BY 4.0 License.

1 Introduction

Ice-nucleating particles (INPs) have a significant impact on climate and weather. They influence cloud formation and thus have an effect on cloud structure, extent and lifetime, as well as on radiation and precipitation properties (e.g. Kanji et al., 2017 and references therein).

Ice formation in the atmosphere can happen via several mechanisms depending on ambient conditions. At temperatures below approximately -38°C, supercooled solution droplets may freeze spontaneously without a crystallization nucleus (homogeneous freezing). To start ice formation at warmer temperatures (T > -38°C), the energy barrier for nucleation has to be reduced. This can be accomplished by the presence of an INP. Conventionally, four mechanisms are distinguished for heterogeneous freezing processes: (1) deposition nucleation, (2) condensation freezing, (3) contact freezing and (4) immersion freezing. Detailed information on ice nucleation terminology can be found e.g., in Vali et al. (2015) and Kanji et al. (2017). The main focus of recent INP-related research has been on the temperature range determined by heterogeneous nucleation which occurs in mixed phase clouds. But INPs may also be important at lower temperature ranges in the cirrus cloud regime, that is often solely associated with homogeneous nucleation (e.g., Murray & Liu, 2022).

Only a small fraction of the total aerosol can act as INPs. In addition to the prevailing environmental conditions (e.g., temperature / humidity), the potential for an INP to become activated is dependent upon various factors, including individual particle properties and its history within the atmosphere. With regard to particle properties, particularly surface characteristics such as imperfections (e.g., cracks, fissures, edges) (Kiselev et al., 2016) and / or specific chemical properties (e.g., functional groups like hydrogen-bridging (Kanji et al., 2008), crystal structure, coating, etc.) can affect the ice-forming capabilities of a particle. These promoting sites on the surface of an INP are termed active sites. As particle size increases, the number of active sites also tends to increase. So typically, the larger an atmospheric particle is, the more likely it is to act as an INP (e.g., Archuleta et al., 2005; Hoose & Möhler, 2012). Moreover, the particle's history in the atmosphere and potential modifications (coating, agglomeration, pre-activation (Abdelmonem et al., 2020)) may be also important factors for activating it. Given the multitude of factors that influence INP activation, it is not surprising that their concentrations show variations of several orders of magnitude in space and time (e.g., Kanji et al., 2017; DeMott et al., 2010). For instance, with a decrease in temperature by a few degrees Celsius, the INP concentration can increase by an order of magnitude or more (e.g., Petters & Wright, 2015; Kanji et al., 2017).

Ice-forming activity has been verified for many atmospheric particle classes. Mineral dust, which is emitted from arid and semi-arid regions and is globally distributed in the atmosphere (e.g., Schepanski et al., 2018; Perry et al., 1997; Ansmann et al., 2003), is an important factor in atmospheric heterogeneous ice formation at temperatures below -15°C (Hoose & Möhler, 2012). The composition of mineral dust is highly variable depending on the source region (Scheuvens & Kandler, 2014). Furthermore, soil dust (mineral dust which is often mixed internally with organic components) from agricultural regions is regarded to be a source of INPs (e.g., O'Sullivan et al., 2014). Metal oxides can be components of mineral dust from natural

https://doi.org/10.5194/egusphere-2024-2797
Preprint. Discussion started: 19 September 2024
© Author(s) 2024. CC BY 4.0 License.

sources and are also emitted by anthropogenic sources. Their efficiency to activate as INPs depends on the type of metallic particle (Kanji et al., 2017). At temperatures warmer than -15°C, mainly biological INPs are ice active (e.g., Kanji et al., 2017; Després et al., 2012). These include primary particles such as bacteria, fungal spore, pollen and plant debris, as well as some biological macromolecules (e.g., Pummer et al., 2012). Particles from biomass burning and fossil fuel combustion are considered as another particle class relevant for ice formation. This includes soot (mostly a mixture of black carbon with organic carbon) as a product of incomplete combustion as well as fly ash from the non-combustible components. However, the contribution of soot to atmospheric ice formation is still subject of discussion, e.g., Cozic et al. (2008) and Kupiszewski et al. (2016) found opposing results at the same location. Besides the continental sources, the oceans also serve as a source for atmospheric INPs. In addition to sea salt, sea spray aerosol also contains increased amounts of marine organic material from the sea surface microlayer, which is considered to have significant ice-nucleating properties (Wilson et al., 2015).
A detailed overview of all atmospherically relevant INPs is given e.g., by Kanji et al. (2017) and Burrows et al. (2022).

Methodically, there are three main approaches to investigate the relevant INP species, their concentrations and role in cloud formation.
(1) In laboratory experiments, selected test aerosols can be activated under controlled conditions. Such experiments can provide important information about the ice-forming properties of individual aerosol types and defined mixtures (e.g., Hoose & Möhler, 2012; Hiranuma et al., 2015; DeMott et al., 2018; Hiranuma et al., 2019).
(2) INPs can be analyzed in field experiments to gain information about their local concentration and to identify particle types and sizes which initiate the ice nucleation process in the atmosphere depending on temperature range, geographic location, etc. (e.g., Wex et al., 2019; Schrod et al., 2020b; Brasseur et al., 2022; Lacher et al., 2024).
(3) Model simulations are of great importance to assess the impact of aerosol on cloud microphysics, estimating cloud-aerosol feedbacks and predicting cloud radiation and precipitation processes. For these modelling tasks it is essential to improve the representation of INPs and their correlation to type-specific aerosol particles in the simulations. The concentration and main chemical composition of aerosol for a given time and location in the troposphere are meanwhile available from models. To relate the main aerosol types to their ice nucleation ability it is therefore necessary to identify the composition of those particles that nucleate ice. Burrows et al. (2022) identified a key need for a closure study that combines size-resolved aerosol composition measurements, particle class dependent INP parametrizations and INP measurements. In order to evaluate the results of such a closure study in the most comprehensive way, the INP measurements ideally contain, in addition to the INP concentration, information on the size and chemistry of the ice-forming particles. However, gaining this desired set of experimental parameters from field measurements is challenging.

Although there is a variety of methods to determine the INP concentration in the laboratory and in the field, only a few of them are simultaneously able to report on the chemical characteristics of individual nucleating particles (Cziczo et al., 2017). In terms of interpreting the results from ice-forming particle experiments, a distinction has to be made between INPs and ice

https://doi.org/10.5194/egusphere-2024-2797
Preprint. Discussion started: 19 September 2024
© Author(s) 2024. CC BY 4.0 License.

residuals (IRs). As defined by Cziczo et al. (2017), INPs are those particles that are activated under defined conditions after the collection of the total aerosol, while IRs are those particles remaining after the evaporation of atmospherically formed ice crystals in clouds. To analyze IRs, ice crystals can be separated directly from clouds by using special inlets (e.g., Schwarzenböck et al., 2000; Mertes et al., 2007; Kupiszewski et al., 2015; Schenk et al., 2014). Analyzing IRs provides information on atmospherically activated particles, but at the same time bears the risk of collecting non-ice-forming particles that have been attached to the ice crystals (Cziczo et al., 2017). By activation of the sampled non-activated total aerosol within an online reaction chamber (e.g., Rogers, 1988) INPs can be identified. To analyze these INPs it is necessary to separate the ice crystals from droplets by one of the previously described inlet systems or a droplet evaporation zone. In both cases, whether direct sampling from clouds (IR) or subsequent activation (INP), the particles' appearances may have undergone alterations due to ice evaporation processes, which could have resulted in differences between the initially activated particle and those analyzed subsequently.

To our knowledge, the only online experiment that has been used to determine all particle groups relevant to ice nucleation simultaneously is single particle mass spectrometry (SPMS) (e.g., Kamphus et al., 2010; Brands et al., 2011; Thomson et al., 2000). In general, online methods allow a real-time analysis with potential high temporal resolution but may have problems at low INP concentrations. However, several studies have reliably demonstrated the coupling between a separation technique and SPMS in a field setting (e.g., Cozic et al., 2008; Pratt et al., 2009; Cziczo et al., 2009; Kamphus et al., 2010; Cziczo et al., 2013; Schmidt et al. 2017; Lacher et al. 2021). Most measurements still rely on indirect information of the supporting aerosol data.

Electron microscopy (EM), as an offline method, offers an alternative approach to study the chemical composition of INPs/IRs. Even though the method cannot provide high temporal resolution measurements due to longer sampling times, it is able to obtain detailed information on morphology and mixing state in addition to chemistry and size of individual INPs and IRs (e.g., Mertes et al., 2007; Prenni et al., 2009; Cziczo et al., 2009; Ebert et al., 2011; Cziczo et al., 2013; Worringen et al. 2015; Eriksen Hammer et al., 2018). For single particle analysis by EM, INPs or IRs are collected on substrates by one of the separation techniques described above. Single particle analysis can be done automated for large data sets or operator controlled (Eriksen Hammer et al., 2019).

This paper describes an offline method for measuring atmospheric INP concentration in combination with a subsequent characterization of the activated INPs. The recently established method couples the ice nucleation counter FRankfurt Ice nucleation Deposition freezinG Experiment (FRIDGE) to a scanning electron microscope (SEM) (a schematic overview is shown in Fig. 1). In this method, particles collected from ambient aerosol onto substrates are analyzed with respect to their ice nucleation ability at various combinations of activation temperature and supersaturation with respect to ice, yielding the INP concentration. The activated INPs can subsequently be characterized by SEM with regard to their properties influencing the formation of ice (chemistry, morphology and size). According to the definition by Cziczo et al. (2017) the analyzed particles are referred to as INPs, even if we characterize them by SEM after activation and evaporation in FRIDGE.

https://doi.org/10.5194/egusphere-2024-2797
Preprint. Discussion started: 19 September 2024
© Author(s) 2024. CC BY 4.0 License.

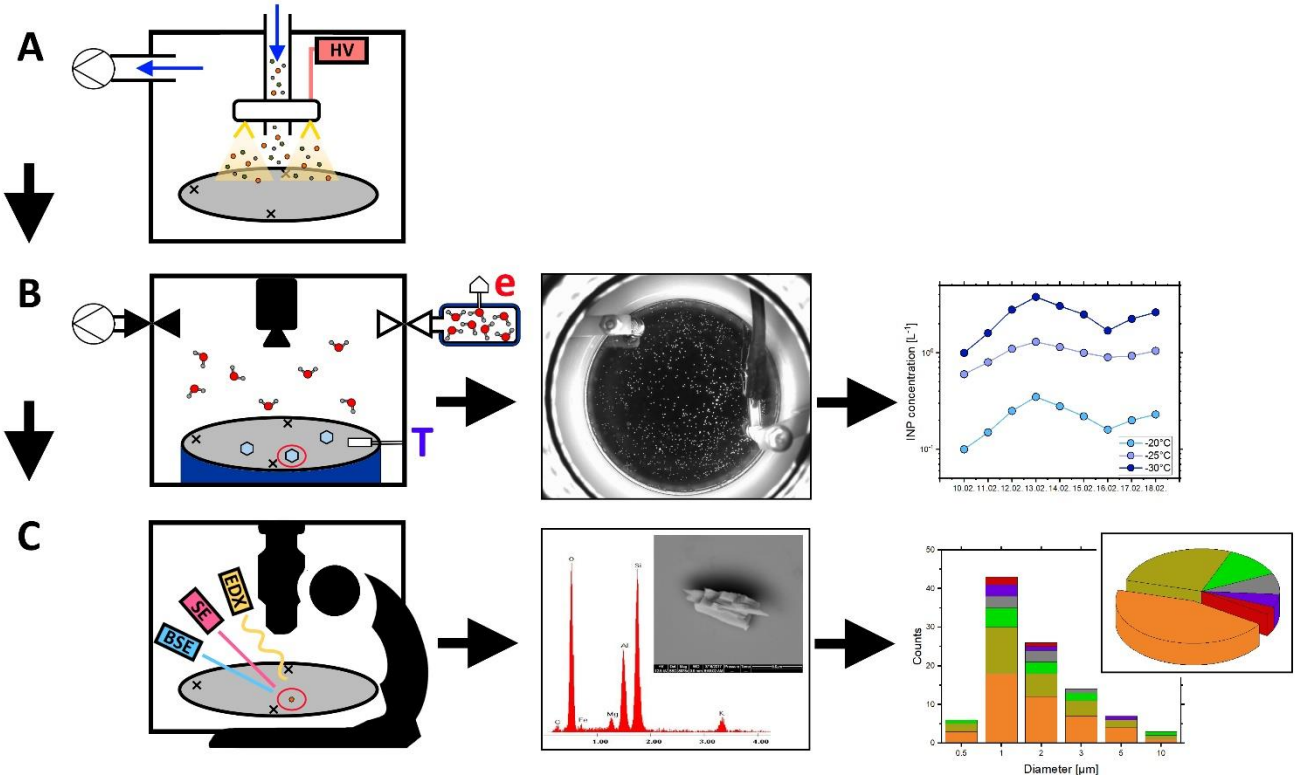

Figure 1: Schematic for the coupled INP analysis. (A) EAC: The aerosol (colored dots) is pumped through the sampling unit in the direction of the blue arrows. By applying high voltage (HV), gold filaments (yellow) arranged in a ring generate an electrostatic field (light yellow triangles). The charged particles are deposited on the silicon substrate (gray). (B) FRIDGE: Diffusion chamber setup with silicon substrate (gray) placed on the cold stage (dark blue) equipped with a temperature sensor (T). The water vapor pressure (e) in the water vapor source (top right) is measured with a pressure sensor. A vacuum pump (top left) is used to evacuate the reaction chamber before the measurement starts. Starting a measurement, the valve to the water vapor source is opened, the diffusion chamber gets flooded with water vapor (red/grey molecules) and ice crystals (light blue) start to grow on the substrate. A camera (top center) monitors the ice growth and records images (see second picture). This can be used to calculate an INP number concentration for different temperature and humidity settings (third picture). (C) SEM: Silicon substrate (grey) with the three engraved crosses defining the coordinate system, placed in the scanning electron microscope (black schematic) equipped with several detectors (solid state detector (blue), Everhart-Thornley detector (red) and energy dispersive x-ray detector (yellow)). Each individual INP which induced ice crystal growth in FRIDGE (particle circled in red) is chemically and morphologically analyzed. The result is a secondary- and backscattered-electron particle image and an elemental spectrum (second picture). As a final result, all the individual particle information is combined in a bulk chemical composition and a chemically resolved size distribution (third picture).

While the FRIDGE-SEM-coupling technique has been used for several campaigns in recent years, providing valuable results (Schrod et al., 2017; Schrod et al., 2020b; Weber, 2019; He et al., 2023), the present publication details the technical procedure. The first part of the paper presents a detailed description of the method, while the second part discusses the results of a case study done at the High-Altitude Research Station Jungfraujoch (JFJ), Switzerland in 2017.

https://doi.org/10.5194/egusphere-2024-2797
Preprint. Discussion started: 19 September 2024
© Author(s) 2024. CC BY 4.0 License.

2 Methodology: Coupling a scanning electron microscope to an ice nucleus counter

2.1 Sample substrates

A silicon disk with a diameter of 45 mm serves as the sample substrate, on which the aerosol particles are deposited by electrostatic precipitation (see Sect. 2.2). The semi-conductive substrate is made from commercially available silicon wafers, which are widely used as basis for microchips in electronic devices. The pure crystalline silicon surface is highly inefficient for ice-nucleation, which prevents from random icing on the wafer, that would induce an artificial background signal and would lead to incorrect INP concentrations. The extremely smooth wafer surface allows for an unambiguous separation of particles from the background in the electron microscope. Each wafer is marked with three laser-engraved crosses near the edge, which span a 90° angle. These markers define a coordinate system, which allows for the precise localization of the ice-nucleation spots (Sect. 2.4).

After analysis, the wafer substrates are cleaned in a simple two-step process and reused subsequently. For this, wafers are pre-cleaned with ethanol and laboratory wipes (Kimtech Science, 7557, Kimberly-Clark) to eliminate oil residues from previous measurements and other coarse contamination. Then, in order to remove fine particles from the surface, the substrates are treated with a beam of dry ice crystals (Sno-Gun II, Va-Trans System, Inc.). The cleaning procedure is performed inside a particle free work space (SPECTEC, laminar flow box FBS). To verify the cleaning process, randomly selected cleaned wafers are analysed in the ice nucleation chamber. However, even after thorough cleaning a small amount of ice formation can regularly be observed at temperatures below -30°C, constituting the background concentration and defining the limit of detection, which is in the order of 0.01 L^{-1} of atmospheric air for a collection volume of 100 L.

2.2 Electrostatic Aerosol Collector

Aerosol is precipitated onto the substrates using an Electrostatic Aerosol Collector (EAC) (Klein et al. 2010, Schrod et al. 2016). Several variants of the collector have been deployed for the use in the laboratory (DeMott et al. 2018), at field campaigns (Lacher et al., 2024, DeMott et al., 2024), for measurements with unmanned aerial vehicles (Schrod et al. 2017) and for long-term observations at research stations (Schrod et al., 2020b). The latter version (PEAC7) is a programmable EAC designed for semi-automated operation of one week of daily sampling.

Inside the collection unit, sample air passes the corona discharge unit, which charges the particles negatively when a high voltage of about 12kV is applied. Charged aerosol particles follow the electric field to the grounded plate and are deposited on the silicon wafer substrate (Fig. 1 A). This sampling process leads to a rather homogeneous particle distribution on the wafer, which is of great importance both for the measurements in the ice nucleation chamber and for the later individual particle analysis by EM. Nevertheless, not all particles are deposited on the wafer during electrostatic precipitation, some are deposited elsewhere in the system. Characterization experiments determined a size-independent collection efficiency of 60 % in the 0.5-3 µm size range. Experimental details and a detailed description of the currently used PEAC7 can be found in Schrod et al. (2016).

https://doi.org/10.5194/egusphere-2024-2797
Preprint. Discussion started: 19 September 2024
© Author(s) 2024. CC BY 4.0 License.

2.3 FRIDGE

The FRankfurt Ice nucleation Deposition freezinG Experiment (FRIDGE) is an offline isostatic vacuum diffusion chamber in which the activation of atmospheric INPs and the associated growth of ice crystals can be observed and documented under laboratory conditions (Klein et al. 2010, Schrod et al. 2016). The diffusion chamber addresses the deposition nucleation and condensation freezing modes but the instrument can also be used in a different setup as a droplet freezing device to address the immersion freezing mode (e.g., Boose et al. 2016; Schrod et al., 2020a). As the immersion mode setup is not subject of our study, the following section describes the measurement procedure for the deposition nucleation and condensation freezing modes (schematic shown in Fig. 1B).

The sample substrate is placed on the cold stage inside the isothermal chamber, and a small amount of silicon oil is applied on the bottom of the wafer to ensure good thermal contact and a homogeneous temperature distribution. For coupling the INP measurement to the single particle analysis, it is important to keep the three laser-engraved crosses on the wafer surface visible during the FRIDGE measurement. The temperature sensor (PT1000) is therefore attached opposite to the middle cross, (see Fig. 1B) also with a little bit of oil. After closing and evacuating the cold chamber, the system is adjusted to selected temperature and humidity conditions. When the selected activation conditions are stable, the valve to the water vapor source is opened and the water vapor diffuses into the cold chamber, activating the INPs on the wafer surface. The growth of ice crystals is observed as a function of time (time step of 10 s) by a CCD camera (2/3" CCD ≥ 5 megapixels, 1 pixel ≈ 400 μm^2) placed above the reaction chamber. Ice crystals are identified by an image analysis software (LabView) comparing the brightness of new objects to a previously recorded reference image. Details can be found in Schrod et al. (2016). For the coupling method it is beneficial to stop the growth of ice before individual ice crystals grow to large sizes or coalescence, because the determination of the ice crystal center, which is assumed to be the position of the INP (see Sect. 2.4.), is more precise with small crystals.

Once a measurement cycle is completed, further measurements can be performed on the same sample under different activation conditions. As a routine, the wafers are measured in 12 cycles combining 3 temperatures (T = -20°C, -25°C, -30°C) and four relative humidity (RH) settings each (RH = 95%, 97%, 99%, 101%). An efficient evacuation between measurement cycles is necessary to ensure the complete water evaporation from the particles to avoid pre-activation effects from residual water / ice in microscopic cavities on the particles surface (Jing et al., 2022). Based on the ice crystal numbers, the collection volume and the PEAK7 sampling efficiency, the INP concentration at different temperature and humidity settings is calculated.

For the subsequent electron microscopy with energy dispersive x-ray spectroscopy, it is important to completely remove the oil from the edge and underside of the wafer after the FRIDGE measurements, as otherwise the chemical analysis of the INPs can be influenced by the evaporating oil. Because of this oil-removing step, the edge and the area of the temperature sensor are excluded from further analysis.

https://doi.org/10.5194/egusphere-2024-2797
Preprint. Discussion started: 19 September 2024
© Author(s) 2024. CC BY 4.0 License.

2.4 Identification of ice crystal position

A homogeneous distribution of ice crystals on the substrate with an adequate range of crystal density is favorable for the coupling process. Furthermore, while working close to RH = 100 %, condensation may occur in the beginning of the FRIDGE measurements. The pictures showing condensation have to be removed, because otherwise the counting algorithm during the position identification is impeded. The steps described below apply to such favored conditions.

The ice crystal positions are identified by image analysis using the internal particle analyzer of ImageJ (Schneider et al., 2012), with a minimum size of 30 pixels proven to be useful. By tagging the centers of the three crosses in a reference image the reference points of the coordinate system are defined manually as their non-uniformity disturbs an automated approach. The ice crystal positions are then tracked through the time series of images, and the image with the maximum number of ice crystals for each measurement cycle is selected for further processing. Based on differences in brightness, the software identifies the ice crystal positions in the images as the center of the detected bright area. After the ice crystal center identification, positions are translated into relative coordinates defined by the calibration marks. Additionally, a calibration image for the electron microscope is generated showing the previously marked center points of the three crosses.

To improve the quality of the data and keep the time-consuming SEM analysis as effective as possible the automatically calculated ice crystal positions are manually inspected to identify erroneous position markings. Therefore, an ice crystal is defined as the following: A clearly visible bright object, which continues to grow in the ice supersaturated regime as the measuring time progresses. Usually, almost all ice crystal positions calculated by the counting algorithm can be confirmed by the manual quality check (Fig. 2). A reason for excluding a calculated coordinate from further analysis is a false identification as a result of ice crystals, which are very close to each other or have grown together. In rare cases, the coordinates of a specific ice crystal may differ slightly between separate measurement cycles due to variations in the extent and symmetry of the crystal growth.

https://doi.org/10.5194/egusphere-2024-2797
Preprint. Discussion started: 19 September 2024
© Author(s) 2024. CC BY 4.0 License.

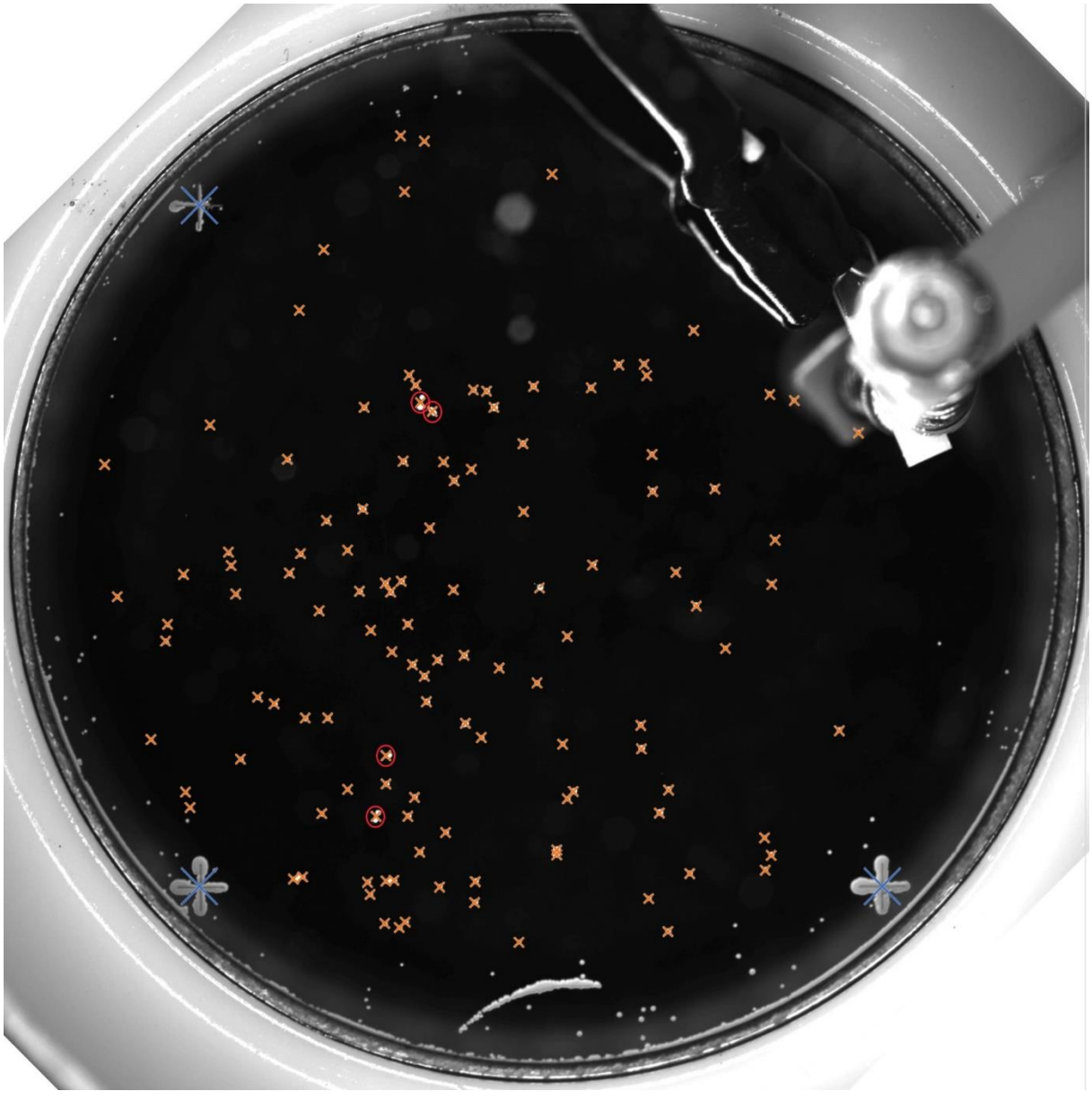

Figure 2: Image of a silicon wafer from the FRIDGE diffusion chamber measurement with grown ice crystals (white dots) and the corresponding calculated positions for SEM (orange crosses). Miscalculated coordinates are marked with a red circle. The three laser-engraved crosses (at the large blue crosses) represent the reference points for the coordinate system. The edge of the sample substrate as well as the area around the temperature sensor are excluded from analysis.

https://doi.org/10.5194/egusphere-2024-2797
Preprint. Discussion started: 19 September 2024
© Author(s) 2024. CC BY 4.0 License.

2.5 Scanning Electron Microscopy

A Quanta 200 FEG Environmental Scanning Electron Microscope (ESEM) by FEI (Eindhoven, Netherlands) coupled to an energy dispersive X-ray detector (EDX) (EDAX, AMETEK, Tilburg, Netherlands) was used for analysis. The instrument is also equipped with an Everhardt-Thornley detector (ETD) which maps the topology of a particle by secondary electrons (SE) and a solid-state detector (SSD), providing the distribution of elements on the particle by backscattered electrons (BSE) giving information on homogeneous or heterogeneous distribution of elements and on inclusions. The EDX provides an elemental composition of an individual particle, which can be used to attribute the analyzed particles to different classes of composition and origin. As all analyses were carried out in high vacuum (10^{-6} mbar), the instrument is referred to as scanning electron microscope (SEM) in the following. The acceleration voltage was 12.5 kV or 15 kV, the working distance was 10 mm as standard.

2.5.1 Coordinate calibration

As the internal SEM coordinate system is centered around the origin in the middle of the stage aligning the axes to the directions of mechanical movements of the stage, it is necessary to perform a coordinate transformation to link coordinates of the SEM to the coordinates defined by the crosses in the previous step. For that, the three crosses on the wafer are used as references in the SEM. It is highly important to locate their centers with high precision, since the position of each ice crystal in the subsequent analysis is based on this conversion. Manual calibration provides the highest precision, as the different physical imaging processes between the two instruments and the high magnification of the electron microscope in contrast to the limited resolution of the FRIDGE calibration picture, impair any precise automated calibration.

2.5.2 Individual particle analysis

Each ice crystal position that has been confirmed by the manual quality check is scanned for particles by SEM. Because the ice crystals are not grown perfectly symmetrical and the FRIDGE images have a limited resolution of about 20 x 20 µm per pixel, the calculated SEM coordinates have an uncertainty. Therefore, a radius of 50 µm around the calculated location is scanned. This radius encompasses the stated uncertainties in order to find the INP while limiting the probability to observe multiple particles in the scanned area. As a result, the method is limited in general with respect to the sampling volume of aerosol. The volume of air to be sampled must balance to effects: it must be sufficiently large to trap a statistically significant number of INPs on a wafer, but must avoid overloading in order to maintain enough distance between all - also the un-activated - particles (total wafer loading) to preserve unambiguity. Consequently, the fraction of INPs to the total aerosol impacts on the possible range of sampled volumes. The method has worked reliably with a standard collection volume in the order of 100 L, despite a possibly high concentration of sub-100 nm particles being present in the sampled air. Presumably, there is a loss of volatile components during our sample collection and processing, enabling higher sampling volumes while limiting the method to the characterization of refractory particles. As the volatile particles are not known to be efficient INPs

https://doi.org/10.5194/egusphere-2024-2797
Preprint. Discussion started: 19 September 2024
© Author(s) 2024. CC BY 4.0 License.

in the considered temperature range (Murray & Liu, 2022), we assume that this loss does not affect the results with respect to the analyzed particles. Since the substrate loading depends strongly on the prevailing total aerosol concentration at the sampling location, the conditions for analysis can be optimized by adjusting the scanning radius for specific circumstances.

While scanning the calculated location, three cases can be distinguished: (1) one particle is found, (2) more than one particle is found, (3) no particle is found.

(1) If a single particle is found within the specified radius, the INP identification is unambiguous and a single particle analysis is carried out. If the BSE-image, in which the contrast depends on chemistry, indicates chemical differences within the particle, multiple EDX spectra of the different areas are recorded. This comprehensive analysis enables the identification of mixing state and distinct morphological patterns on the particle surface that may be pertinent to ice formation.

(2) If more than one particle is found in the defined area around the coordinate these positions are usually excluded from analysis. In case all particles in the scanning area have the same chemical composition, the information about the particle class relevant to ice formation is still obtained. However, no clear statement on the size and specific features of one unique INP can be made.

(3) If no particle is found within the 50 µm radius, these blank positions are usually neglected as well. However, if the substrate loading is low, extending the screening radius (e.g., to 100 µm) in case of a blank position can help to increase the number of identified INPs. It is important to consider this extension for the entire sample, otherwise the unique identification criteria of an INP are no longer consistent.

Depending on the total wafer loading, the number of INPs identified by SEM is usually smaller than the number of ice crystals grown during the FRDIGE measurement.

The size of each identified INP is determined by calculating the projected area diameter (d_{pa}) from the SE- / BSE-images. Therefore, the particle is regarded as an ellipse and the dimensions of its major and minor axis are determined in order to subsequently calculate the diameter of an equivalent circle, which is referred to as d_{pa}. The calculated diameters represent the particle size obtained as a result in the last stage of the analysis and may therefore differ from the size of the initially activated INPs. Volatile components within a sample (e.g., water) may evaporate during the analysis procedure possibly changing the appearance of the sampled particles. Figure 1 C shows a schematic of this SEM-step with a BSE-image / EDX spectra and the chemically resolved size distribution as a final result.

2.6 Chemical classification

The analysis by SEM and EDX is an excellent way of characterizing INPs in detail, as in addition to the chemical analysis, which provides information about the elemental composition of an INP, the morphological characterization can be used to identify surface properties relevant to ice nucleation. In our specific case, the silicon content cannot be quantified as we are working on a Si substrate and we therefore always obtain a Si background signal in the spectrum. In the case of very small particles the signal intensity with respect to this background signal may be too weak or missing, so there is no possibility to

https://doi.org/10.5194/egusphere-2024-2797
Preprint. Discussion started: 19 September 2024
© Author(s) 2024. CC BY 4.0 License.

characterize them chemically. The same applies for particles with an original droplet shape as well as for residues that spread more like a film. Instability with respect to the electron beam also leads to limited detection of particle properties.

In the following section we define the particle classes which were used to categorize the identified INPs sampled at the high-altitude research station Jungfraujoch in winter 2017 (see Sect. 3). In the following we present a brief description of each group, focusing only on the major elements and properties. As the particle composition depends on the sampling location, the INP classification scheme (supplementary material – Fig. S1) for other locations may be different.

Mineral components

The *aluminosilicate / Al-rich* group includes all particles which have aluminum (and oxygen) as their main detectable elements – due to the Si-wafer substrate, there is always a large peak from Si present which cannot be quantified. Nearly all particles contain several minor elements in different ratios (e.g., Na, Mg, K, Ca, Fe), depending on the minerals from which they originate. Most particles are irregular and their internal element distribution is not homogeneous. The dominating source for aluminosilicates in the atmosphere is mineral dust from arid and semi-arid regions, while Al-dominated particles are usually rare (e.g. Okada & Kai, 2004; Kandler et al., 2007).

The spectra of the *carbonate group* include, in addition to carbon and oxygen, calcium and/or magnesium as counterions. The irregular shaped particles can be related to geogenic origin (e.g., calcite, dolomite).

If only oxygen can be detected alongside silicon, it can be assumed that it is *silicon dioxide* (quartz), however it is not possible to make a reliable statement about the silicon content of the particles. Most geogenic quartz particles show irregular shapes with typical sharp edges (Whalley and Krinsley, 1974). Anthropogenic SiO_2 particles from industrial high temperature processes show more spherical shapes. Fragments of the wafers are clearly identified as artifacts by their sharp edges, glassy fracture and lack of oxygen signal.

Carbon containing particles

In addition to a high carbon content, the group of *biological particles* is characterized by the presence of biogenic trace elements such as phosphorus, potassium, magnesium, calcium, sodium, etc. (Ebert et al. 2000) and by their characteristic appearance. Based on our criteria, particles are only classified as biological if the bulk particle fulfills these criteria. The group of biological particles includes plant debris, pollen, bacteria and fungal spores as well as their fragments.

In many cases, *soot* particles can be clearly assigned based on their typical morphology, which often shows long chains or larger agglomerates of small, spherical primary particles (Sorensen & Feke 1996). Due to particle aging in the atmosphere or small particle sizes some of the soot particles cannot be classified by their morphology. In these cases, they have to be characterized by their very low oxygen content compared to carbon. All particles with a high carbon content, which cannot be classified as soot by the previous criteria are classified as C-rich. The proportion of soot therefore only represents a lower limit.

https://doi.org/10.5194/egusphere-2024-2797
Preprint. Discussion started: 19 September 2024
© Author(s) 2024. CC BY 4.0 License.

The *C-rich group* contains all particles with high carbon peaks in their spectra, which cannot be clearly classified as biological particles or soot. Since some particles from those two groups can be assigned as C-rich, this class may contain also components from all other refractory organic parts in the atmosphere. Therefore, the morphological variability of these particles is high.

Other particle classes

The *metal oxides* are characterized by the presence of oxygen and a corresponding metal not classified into a previous group, which is in our case primarily iron. The morphology of these particles can be either irregular (e.g., natural mineral durst, anthropogenic urban dust), or spherical, with the latter possibly originating from high-temperature processes (e.g., coal combustion) or aircraft emissions. Since no final source identification of the metal oxides could be performed, we refrain from clearly assigning this group to a mineral origin.

The particles of the *sulfate group* are mainly characterized by the presence of sulfur and oxygen. Calcium and, in some cases, potassium are the primary counterions. The appearance of these particles varies from clean crystallization to agglomerates and irregular shapes, depending on their source and formation processes. Besides the geogenic sources (minerals like gypsum or anhydride), possible anthropogenic sources are industrial processes (mainly coal combustion), flue gas desulfurization and fertilizers. This method can detect only beam-stable sulfates reliably. Ammonium sulfate, for example, is not beam-stable during the analysis and therefore cannot be detected reliably. Due to the diversity of their possible sources and characteristics, we abstain from classifying them as minerals.

The group of *mixtures* includes particles which are containing elements from more than one of the groups presented. The most abundant mixtures feature in addition to an Al peak, which is characteristic for the aluminosilicate / Al-rich group, also a distinct carbon peak (C/Al-ratio > 0.2). This can be an indication of soil dust, which contains carbonaceous material in addition to aluminosilicate / Al-rich minerals. Apart from this, the described composition can also be generated by mixing or coating with carbonaceous materials during particle aging in the atmosphere. The morphology of the particles is as variable as the composition and is mostly irregular.

In rare cases, traces of gold were found on single particles. Since gold wires are used as electrodes to initiate the discharge during the sampling process, these particles were categorized as sampling *artifacts* and therefore excluded from further analysis.

All particles which can be clearly identified as INPs based on their position, but do not provide clear element peaks beside the silicon background signal are grouped as *not classifiable***.**

An overview of all particle groups with example pictures and EDX spectra is given in Fig. 3.

https://doi.org/10.5194/egusphere-2024-2797
Preprint. Discussion started: 19 September 2024
© Author(s) 2024. CC BY 4.0 License.

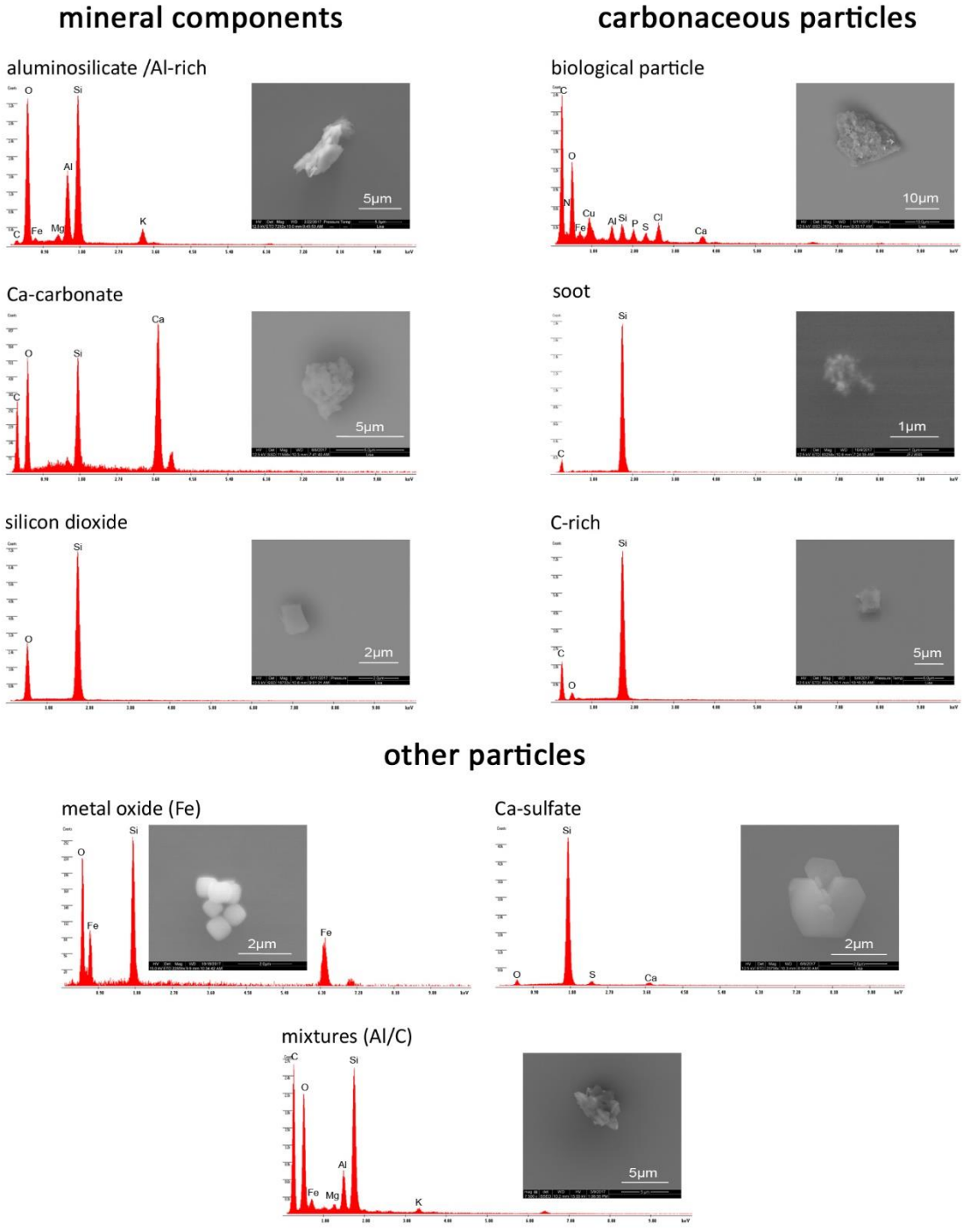

375 **Figure 3: Overview of representative EDX spectra and corresponding SE- / BSE-images for each particle class from CLACE / INUIT 2017 at the high-altitude research station Jungfraujoch.**

https://doi.org/10.5194/egusphere-2024-2797
Preprint. Discussion started: 19 September 2024
© Author(s) 2024. CC BY 4.0 License.

3 Case Study: Results from the CLACE / INUIT campaign at the high-altitude research station Jungfraujoch in 2017

3.1 Sampling site

The high-altitude research station Jungfraujoch (JFJ) is located in the Swiss Alps at 3580 m above sea level between the mountain peaks of Mönch and Jungfrau. A general description of the station can be found in Bukowiecki et al. (2016). The samples were collected during the Cloud and Aerosol Characterization Experiment / Ice Nucleation Research Unit campaign (CLACE / INUIT 2017) between January 21 and February 25 2017. During winter, the station is 60% of the time in the free troposphere (FT) (Herrmann et al., 2015), which enables characterization of the global background aerosol. A temporary influence of the planetary boundary layer is possible at any time of the year. According to Baltensperger et al. (1998) the station is in clouds (mixed-phase and ice) 40% of the time. Since the average temperature did not fall below -15°C during the sampling period, we assume that most INPs with activation temperatures of -20°C to -30°C were not activated under the prevailing environmental conditions. Even though some of them might have been activated previously in higher clouds, sampling under cloudy conditions likely does not introduce a large bias due to previously activated INPs.

3.2 INP concentration

Since the INP concentration for -20°C and -25°C was sometimes very low during the campaign (Fig. 4), we focus on the INPs activated at -30°C (c_{INP-30}) for the single particle analysis.

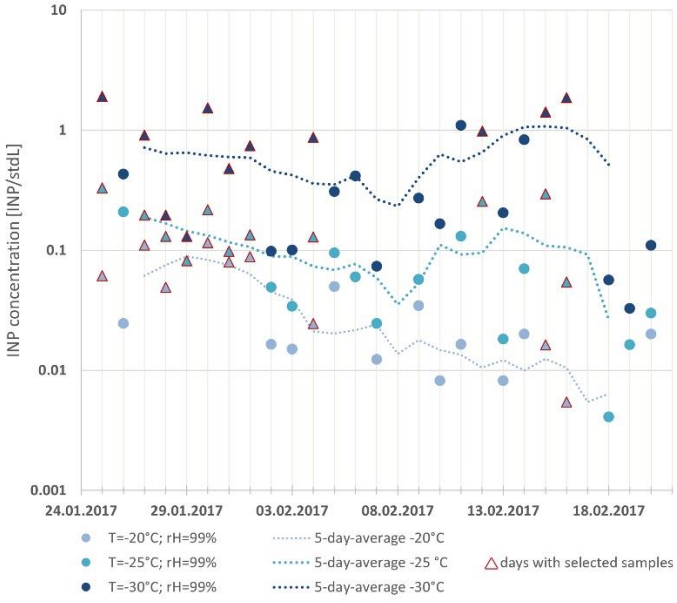

Figure 4: INP concentrations (deposition nucleation / condensation mode freezing) calculated from the FRIDGE measurements at RH = 99 % (for days with more than one sample, an average value was calculated). Days with analyzed samples are indicated by triangles and the corresponding sample numbers. The 5-day-average concentration is shown by the dotted lines (the figure was modified according to Weber (2019)).

https://doi.org/10.5194/egusphere-2024-2797
Preprint. Discussion started: 19 September 2024
© Author(s) 2024. CC BY 4.0 License.

The c_{INP-30} varied between 0.1 and 1 $stdL^{-1}$ for most of the campaign. A Saharan dust event (SDE) was encountered during the end of the campaign. The INP concentrations for -25°C and -30°C followed the same trend in general, including a marked increase in the INP concentration during the SDE. This was not the case for -20 °C, because Saharan dust particles primarily activate as INPs at temperatures below -20°C. 14 substrates out of a larger set of samples from the measurement campaign were analyzed with the here presented method. The particular samples were chosen because of their ice crystal abundance and homogeneous distribution on the substrate during the FRIDGE measurements. These samples are indicated by the corresponding sample number and triangles in Fig. 4. Based on the experience that most ice nuclei active at warmer temperatures also activate at colder temperatures, it can be assumed that only a few INPs are neglected due to limiting the analysis to INPs activated at -30°C.

3.3 Method evaluation

Between 8 and 220 ice crystals had grown on the substrate surface of each wafer during the ice nucleation experiments in FRIDGE at -30°C. Figure 5 shows a comparison between the number of ice crystals counted by FRIDGE and the number of ice crystal positions calculated for the SEM analysis as described in chapter 2.4.

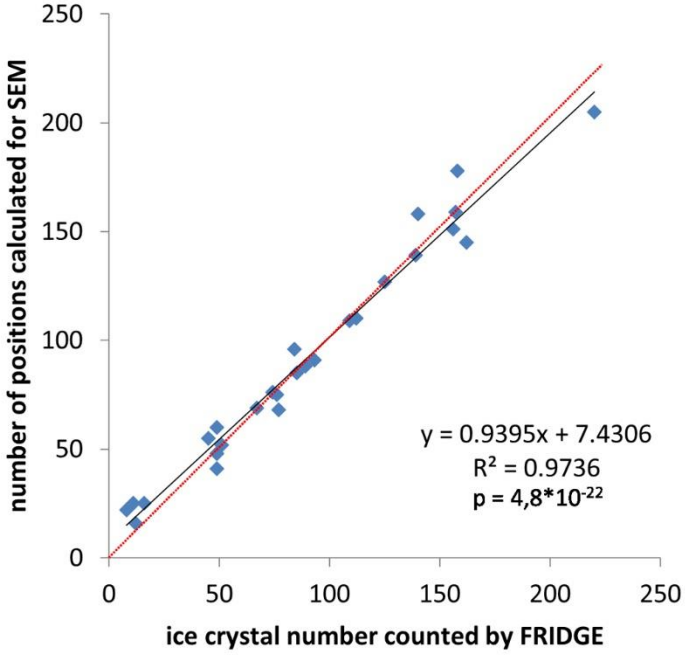

Figure 5: Comparison of ice crystal numbers detected by FRIDGE with the number of positions calculated for SEM analysis for the samples from CLACE/INUIT 2017 at the high-altitude research station Jungfraujoch (activated at T = -30°C and RH = 95 / 97 / 99 / 101 %).

https://doi.org/10.5194/egusphere-2024-2797
Preprint. Discussion started: 19 September 2024
© Author(s) 2024. CC BY 4.0 License.

In most cases, the numbers are almost identical, the few deviations are caused by various reasons. Higher numbers calculated for SEM are mainly caused by the counting of areas with condensation or by an incorrect wafer positioning in FRIDGE, resulting in counting ice crystal growth at the temperature sensor, which is normally excluded by the counting algorithm. A lower number of ice crystal positions calculated for SEM is often caused by ice crystals that have grown together due to prolonged measurement in FRIDGE, resulting in only one position for two crystals. Further improvements in the calculation of individual ice crystal positions can be achieved by specifically avoiding the sources of error previously mentioned.

In the end, based on the parameters described in Sect. 2.5.2., we were able to clearly identify and characterize the associated INPs for 200 ice crystals, which is a fraction of 15% of the total number of ice crystals grown on the 14 wafers. Unfortunately, at the time of the study, only a restricted area of 4 cm^2 in the middle of the wafer was analyzed by SEM, which corresponds to about half of the total analyzable area. Due to the oil removal process that has to be done before SEM, the edge of the wafer and the aera of the temperature sensor have to be excluded. Taking the whole analyzable area into account, the unambiguous INP identification rate can be calculated at 30% for this campaign. We found more than one particle at 40% of the locations, at the remaining 30% we found blank positions. As these numbers depend strongly on the total wafer loading, which correlates to the total particle concentration and the activated fraction in the sampled volume as explained in Sect. 2.5.2., the identification rates given above apply only for the specific conditions encountered during the CLACE / INUIT 2017 campaign. In more recent studies, the area of analysis has been extended to the total analyzable wafer surface, to increase the total number of identified INPs, yielding better statistics.

3.4 INP chemistry

Figure 6 shows the total chemical composition of the INPs over the entire campaign period. Due to the limited number of identified INPs per sample, a detailed meteorological interpretation of results is not feasible. Included are samples from both cloudy and clear sky, as well as air masses from different regions and a SDE. The INP chemical composition of the individual samples can be found in the Supplementary Material (Fig. S2).

mineral components	
aluminosilicates / Al-rich	50 %
carbonates	10 %
silicon dioxide	3 %
carbon containing material	
biological particles	1 %
soot	1 %
C-rich	12 %
other	
metal oxides	4 %
sulfates	2 %
mixtures	13 %
not classifiable	4 %

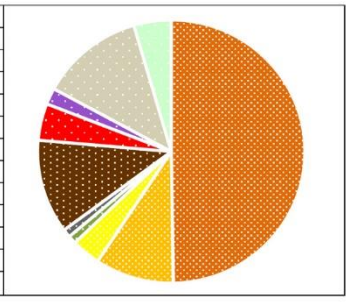

Figure 6: Total chemical INP composition (artifact excluded; n = 199) from CLACE/INUIT 2017 at the high-altitude research station Jungfraujoch (activated at T = -30°C and RH = 95 / 97 / 99 / 101 %).

https://doi.org/10.5194/egusphere-2024-2797
Preprint. Discussion started: 19 September 2024
© Author(s) 2024. CC BY 4.0 License.

Mineral components

The analyzed INPs sampled at JFJ in January and February 2017 were dominated by mineral components (in total 63 %). Among these, the *aluminosilicate / Al-rich group* was prevalent with 50 % and was detected in all individual samples (except W10, which had only one identified INP in total). Very high abundances of these geogenic aluminosilicate / Al-rich particles were found especially for three samples taken during the SDE (W34 / W42 / W45) but also for two samples before the SDE (W2 & W17). Beside Al and Si, mostly Fe, K, Mg, C and Na showed up as minor elements. *Carbonate* particles were detected in 9 individual samples (total contribution of 10 %) with Ca as the main counter ion. Two carbonates showed indications of former droplet shape, suggesting that they originally existed as airborne droplets. *Silicon dioxide* particles contributed 3 % of all identified INPs. Particles with irregular shapes were found in three samples, all spherical particles derived from one sample (W45). Since spherical particles mostly originate from high temperature processes, maybe this sample was influenced by an anthropogenic SiO_2 source (regional or long-range transport).

Carbon containing particles

The carbon-dominated particles represented 14 % of the total INP composition during the CLACE / INUIT 2017 campaign. Only a very small percentage (1 % in each case) could be clearly assigned to a biological origin or soot. The remaining 12 % were classified as C-rich, and both biological fractions and soot, as well as any other carbonaceous particles existing in the atmosphere, may be included in this group.

Other particle classes

During the CLACE / INUIT 2017 campaign at the high-altitude research station JFJ *metal oxides* were found in 5 samples (4 % in total). These were primarily iron oxide, but some single oxides with other metal ions (magnesium and zinc) have also been detected. A few particles within this group contained iron together with Ni and Cr as alloying elements that could be characteristic for steel. An anthropogenic origin or a local source from the station for these particles is assumed, but not confirmed. Apart from some single metal oxides with spherical shapes, most of them showed irregular shapes.

Sulfates were rare (2 %) and only present in three samples with Ca as the main counterion. The potassium sulfate appeared to be droplet-shaped, indicating that it was originally present as a droplet in the air.

The *mixed particles* group contained 13 % of all identified INPs. Besides two metal oxides with additional carbon signals and two particles with signals from Fe and S, the other mixed particles showed element signals from aluminosilicate / Al-rich particles (Al as a tracer in combination with characteristic minor elements) but also a distinct signal for carbon. Most of this Al/C-mix INPs had stronger Al-Peak with respect to the carbon peak (C/Al-ratio < 1). In contrast to the aluminosilicate / Al-rich group these Al/C-mixed particles were found primarily in samples without influence of the SDE, potentially pointing to a different origin of the air masses and thus a different type of mineral material (e.g., soil dust) which was transported to

https://doi.org/10.5194/egusphere-2024-2797
Preprint. Discussion started: 19 September 2024
© Author(s) 2024. CC BY 4.0 License.

the station. Another possible reason could be that the particles have been processed during their atmospheric exposure and, in contrast to the freshly emitted Saharan Dust, are mixed with other carbonaceous components.

For 4 % of all clearly localized particles no chemical classification could be performed as outlined in Sect. 2.5.2.

Comparison to IR measurements from CLACE / INUIT 2017

Our results for INPs activated in the deposition nucleation and condensation freezing modes at -30°C can be compared to IR measurements which were done during the same CLACE / INUIT 2017 campaign by other groups using Ice Counterflow Virtual Impactor (Ice-CVI; Mertes et al., 2007) as separation technique and different analyzing methods.

Eriksen Hammer et al. (2018) found similar particle classes as is presented here for their IRs collected between -10°C and -18°C and analyzed by SEM. Due to different activation conditions, freezing modes and sampling times, it is not possible to make detailed comparisons of the abundances of individual groups. For instance, soot is only activated as INP at very low temperatures, which explains the low abundances detected at - 30°C and its absence at warmer conditions as observed by Eriksen Hammer et al. (2018). Additionally, they sampled the total aerosol to investigate the enrichment or depletion of individual substances. In contrast to the composition of IRs, the total aerosol was primarily composed of complex secondary particles. As previously mentioned, our method is unable to detect these partially volatile compounds. However, their absence does not appear to significantly impact ice nucleation within the analyzed temperature range, thus not affecting the validity of our method.

Lacher et al. (2021) characterized IRs using the Aircraft-based laser ablation aerosol mass spectrometer (ALABAMA; Brands et al., 2011)). Consistent with our results and those by Eriksen Hammer et al. (2018), the dominant fraction was mineral dust (Al-rich + mineral dust) with a 58% abundance. Many mineral dust particles showed signals of biological material, which may be equivalent to the INPs in our study that exhibited a mixture of mineral and carbonaceous components. The lower percentage of mixed mineral particles in our case may be due to colder activation temperatures during the FRIDGE measurement, where activation of pure minerals is more likely. Metals, biological particles, and elemental carbon were also found in a similar percentage as in our distribution. However, since the classification of the particles followed a different scheme, the remaining groups cannot be directly compared.

Comparison to INP/IR measurements from previous studies at the high- altitude research station JFJ

The chemical composition of INPs presented here is in good agreement with previous studies conducted at the high-altitude research station JFJ. However, due to the use of different methods, only a rough comparison can be made among the main particle classes.

Mineral components have already been identified by earlier studies as an important feature of IRs at JFJ. Kamphus et al. (2010) reported a significant enrichment of mineral dust in IRs compared to the total aerosol (57 % compared to 17 %), using Ice-CVI and mass spectrometry. Worringen et al. (2015) also found terrigenous material as the main component in

https://doi.org/10.5194/egusphere-2024-2797
Preprint. Discussion started: 19 September 2024
© Author(s) 2024. CC BY 4.0 License.

their INPs and IRs analyzed by SEM. Depending on the sampling technique, the values were ranging from 32% to 55%. The magnitude of both results agrees well with our mineral dust proportions in INPs.

Carbonaceous material was also identified as INPs / IRs at JFJ during winter 2013 by Worringen et al. (2015). The relative number abundances for these particles are in good agreement with our measurements for two of the three sampling methods they used (Ice-CVI, Ice Selective Inlet (ISI) and Fast Ice Nucleus Chamber (FINCH) + Ice Nuclei Pumped Counterflow Virtual Impactor (IN-PCVI)). The authors suggest that the higher proportion of carbonaceous particles observed with ISI is likely due to the collection of different air masses at the end of the campaign.

Metallic particles and metal oxides have also been identified as ice-forming compounds in previous studies conducted at JFJ. Kamphus et al. (2010) reported the presence of 14 % metallic particles in their IRs, but their classification scheme is not directly comparable to ours. Ebert et al. (2011) collected IRs by Ice-CVI separation to study them with EM. They also found metal oxides in their IRs and classified them primarily as iron oxide, which is consistent with our results. Worringen et al. (2015) also reported the existence of metal oxides in IRs and INPs, with relative number abundances ranging from 5% to 20 %. Our calculated fraction of 4 % agrees well with their lower limit.

A clear enrichment of complex mixtures in the IRs compared to the total aerosol was found by Ebert et al. (2011). Half of the particles in this group were described as silicate mixture particles that mainly contained carbonaceous material as well. This corresponds to our mixed group. Such a silicate mixture group was also defined by Worringen et al. (2015), in relative proportions corresponding to what we have found.

3.5 Chemically-resolved INP size distribution

In addition to providing information on the concentration and chemical classification of INPs, our coupling method also yields data on their size. This is a significant advantage in creating an INP size distribution, as it offers information about the chemical composition of each individual size bin.

Figure 7 shows the chemically resolved size distribution of all identified INPs from the CLACE / INUIT 2017 campaign at the high-altitude research station JFJ. The graph displays the absolute INP numbers within a specific size range, with the maximum found between 1 µm and 2 µm. In comparison to a total aerosol size distribution from the FT at JFJ (e.g., Nyeki et al., 1998), the maximum of the INP size distribution is significantly shifted towards larger diameters. We hypothesize that, in addition to the primary suitability of larger particles as ice nuclei, the volatility of the small aerosol components (nitrates, sulfates, and organics) may play a role here. As mentioned above, these volatile compounds cannot be detected by our coupling technique, which is why this method is limited to the analysis of non-volatile substances.

https://doi.org/10.5194/egusphere-2024-2797
Preprint. Discussion started: 19 September 2024
© Author(s) 2024. CC BY 4.0 License.

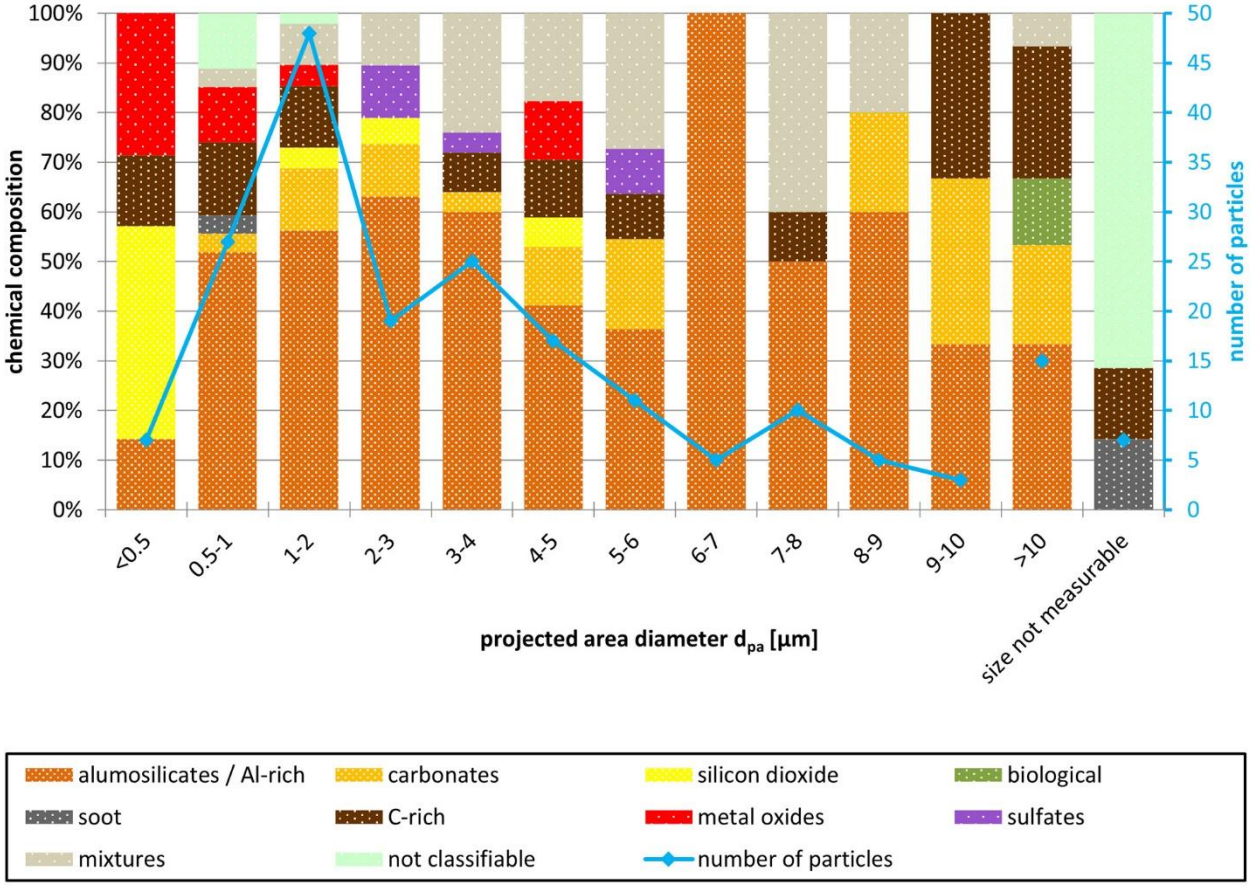

Figure 7: Chemically resolved size distribution for all identified INPs (artifact excluded; n=199) from CLACE/INUIT 2017 at the high-altitude research station Jungfraujoch (activated at T = -30°C and RH = 95 / 97 / 99 / 101 %).

As the mineral particles (aluminosilicates / Al-rich, carbonates and silicon dioxide) are in general the most prevalent group within the analyzed samples, they are also the most prevalent group in all size ranges, with proportions ranging from 50% to 100%. The proportions of the individual components vary for the different size ranges.

Only 3 % of the analyzed INPs had a quantifiable diameter smaller than 0.5 µm. The smallest INP whose size could be determined with confidence was 300 nm, although we can generally also see smaller particles in the SEM. This agrees to well-established findings in literature that most particles only act as effective ice nuclei above a size of 500 nm (DeMott et al., 2010). Besides the mineral particles, which primarily consist of silicon dioxide (both spherical and non-spherical), the smallest size bin shows the highest proportion of metal oxides (non-spherical).

https://doi.org/10.5194/egusphere-2024-2797
Preprint. Discussion started: 19 September 2024
© Author(s) 2024. CC BY 4.0 License.

Significantly more particles (14 % of all identified INPs) were found in the size range between 0.5 µm and 1 µm. The mineral fraction is manly composed of aluminosilicates / Al-rich particles, with a small number of carbonates. Additionally, soot and C-rich particle as well as metal oxides and mixtures can be assigned to the second size bin. However, due to their submicron size, some particles could not be chemically classified.

The size range of 1-2 µm contained the largest number of INPs (24 % in total). Again, aluminosilicates / Al-rich particles are the most abundant group in the mineral fraction. Additional contributions from carbon containing particles, metal oxides and mixtures are reported.

The number of particles decreases for INPs with d_{pa} > 2 µm, which is consistent with a reduced residence time in the free troposphere as particle size increases. Besides the mineral fraction, which is mainly represented by Aluminosilicates / Al-rich particles and carbonates, the proportion of mixtures increases notably for INPs larger 2 µm. C-rich particles are also found to be distributed over the entire size range up to 10 µm. All sulfates can also be found in this range.

Since the abundance of INPs with d_{pa} > 10 µm is low (8 %), they are summed up. The largest INP had a d_{pa} of 34.5 µm. Due to sedimentation, long-range transport of these large particles is very unlikely. However, a local influence by air that is advected from the planetary boundary layer to the station cannot be excluded. Besides mineral particles and C-rich particles, the two biological particles were also found in this size range.

No d_{pa} could be determined for some C-rich and soot particles, as well as for most particles without a chemical classification, since they were mostly too small to get a usable image.

Note the relatively high statistical uncertainty due to the low INP numbers.

Lacher et al. (2021) measured the size distribution of IRs during CLACE / INUIT 2017 downstream of an Ice-CVI using an optical particle counter with a size range of 0.3-5 µm. The highest concentration was found for IRs with a diameter of 0.3 µm. The secondary broad maximum with diameters between 1.3 µm and 5 µm agrees reasonably well to our findings. Comparing the chemically-resolved size distribution of IRs analyzed with ALABAMA to what is presented here is difficult because the majority of IRs analyzed by Lacher et al. (2021) were smaller than 1 µm.

Worringen et al. (2015) also determined size distributions (maximum particle size 3 µm) for their major INP/IR components. In each of their three different sampling setups, the maximum particle number was found to be between 0.3 and 0.5 µm diameter. The particles collected with ISI showed a second maximum at 1 - 1.5 µm, which is the same range as our maximum. Terrigenous particles, including silicates and Ca-rich particles, were primarily found in the larger size ranges, while carbonaceous particles/soot and metal oxides were predominantly detected in the submicron range. In our results, both the metal oxides and the few soot particles also showed very small diameters, while the mineral components were distributed over all size ranges. In contrast to Worringen et al. (2015), our C-rich particles were present over the entire size range. The reason for this is possibly that our classification scheme assigned the larger potentially biological particles as C-rich.

The shift towards larger particle diameters in our results in comparison to the maxima from Lacher et al. (2021) and Worringen et al. (2015) may be caused by the differences in sampling and ice activation. When collecting IRs using any type

https://doi.org/10.5194/egusphere-2024-2797
Preprint. Discussion started: 19 September 2024
© Author(s) 2024. CC BY 4.0 License.

of counterflow virtual impactor, there is always a size selection of the ice crystals, which indirectly affects the resulting INP/IR size distribution. INPs in FRIDGE are activated through deposition nucleation / condensation freezing under defined conditions, while the IRs collected from ambient air are activated under natural and even more complex conditions, including the potentially more important immersion freezing mode (Lohmann et al., 2016).

4 Summary and conclusions

A method for analyzing the concentration and individual physico-chemical properties of ambient INPs has been developed. The method benefits from the coupling of two instruments already used for the analysis of INPs and IRs: the static diffusion chamber FRIDGE and the SEM. This coupling allows for detailed analysis of various INP properties, such as chemical composition, mixing state, size, morphology, and surface properties like cracks or pores.

In this study ambient atmospheric aerosol samples were collected onto silicon wafer substrates using a simple electrostatic precipitator setup. Deposition nucleation and condensation freezing mode INPs were activated and photographed in the static diffusion chamber FRIDGE at several combinations of temperature and humidity. Engraved calibration marks were used to transfer the center point coordinates of the ice crystals grown in the FRIDGE experiment to the electron microscope. It was shown, that this position calculation works reasonably well, with a neglectable number of misplaced positions. Observing every single ice crystal origin using a SEM with an EDX detector provided the opportunity to comprehensively analyze the properties of individual INPs at each position where only one particle was found. A size distribution of the number and composition of INPs can be achieved. The identification rate was calculated at 30 % for the presented field data, but may vary for other samples, as it depends strongly on the total wafer loading. By using position data sets from different sets of activation conditions, future studies may relate the composition and sizes of INPs to the different activation conditions. This may help to identify which particle types and features are atmospherically most relevant as a function of temperature. However, due to the relatively low counting statistics, further improvements are necessary to obtain a more reliable insight into the relevance of the particle properties for the INP activation.

The presented analysis of INPs collected at the high-altitude research station JFJ in winter 2017 demonstrates the benefits of coupling FRIDGE to the SEM. The results are generally comparable to ones from other methods, partially obtained at the same location or even within the same campaign. However, the size distribution obtained by this technique differs from others, which may be related to the sampling mechanism and activation conditions.

The mineral components, mainly aluminosilicates / Al-rich particles, but also carbonates and silica, were clearly dominant as INPs in the predominantly free tropospheric air masses at the JFJ. These components originated primarily from non-local background dust sources - and specifically from a Saharan dust event. They were distributed over the entire size range, except for silicon dioxide, which was mainly found in the size range below 500 nm. We found carbonaceous INPs of various sizes, including a minute amount of small soot particles as well as large biological particles. Additionally, a small amount of

https://doi.org/10.5194/egusphere-2024-2797
Preprint. Discussion started: 19 September 2024
© Author(s) 2024. CC BY 4.0 License.

metal oxides, mostly iron oxide, with primarily $d_{pa} < 500$ µm were also identified. Sulfates were rare. Mixed particles, predominantly aluminosilicate / Al-rich particles with increased carbon content, were more frequently found at larger diameters.

The results from several campaigns (Schrod et al., 2017; Schrod et al., 2020b; Weber, 2019; He et al., 2023) consistently demonstrate the potential of coupling the two instruments for the detailed analysis of deposition nucleation / condensation freezing mode INPs. This method can also determine ice activity for particles with a size of several micrometers, making it a useful complement to methods with size restrictions due to inlet systems or other factors. Together with the structural information that can be obtained from SEM, it can be a valuable addition to pure INP counting methods for gaining information on the relevance of particle properties to ice nucleation efficiencies. The resulting information about the physico-chemical properties of individual INPs could help to bridge the knowledge gap towards INP aerosol-type-specific parametrizations that could be used in modeling studies.

As experimental knowledge about concentration and composition of INPs, and their contribution to upper tropospheric ice nucleation processes in cirrus cloud formation is severely lacking (Kanji et al., 2017), the method will be adapted for future aircraft campaigns.

Data availability

The complete data set is available for the community and can be accessed by request to Lisa Schneider (schneider@geo.tu-darmstadt.de) or Martin Ebert (mebert@geo.tu-darmstadt.de) of the Technical University Darmstadt.

Author contributions

The concept of the study was designed by JC, ME and HB. The samples at the high-altitude research station Jungfraujoch were collected by DW, who also performed the FRIDGE measurements and interpreted the INP concentration data with HB, JC and JS. The scanning electron microscopy analysis was performed by LS, the interpretation was done with support from ME. KK wrote the program to perform the ice crystal center determination and coordinate conversion. The general method evaluation was done by LS, KK, HB, JS, ME. The paper concept was drafted and written by LS and JS, with contributions from DW, HB, JC, ME and KK.

Competing interests

One Co-author is member of the editorial board of the journal Atmospheric Measurement Techniques.

Acknowledgements

This work was funded by the Deutsche Forschungsgemeinschaft (DFG, German Research Foundation) – TRR 301 – Project-ID 428312742 and by the Ice nucleating research unit INUIT (FOR 1525 (project ID 170852269)).

https://doi.org/10.5194/egusphere-2024-2797
Preprint. Discussion started: 19 September 2024
© Author(s) 2024. CC BY 4.0 License.

References

Abdelmonem, A., Ratnayake, S., Toner, J. D., Lützenkirchen, J.: Cloud history can change water-ice-surface interactions of oxide mineral aerosols: a case study on silica, Atmos. Chem. Phys., 20, 1075-1087, doi:10.5194/acp-20-1075-2020, 2020

Ansmann, A., Bösenberg, J., Chaikovsky, A., Comerón, A., Eckhardt, S., Eixmann, R., Freudenthaler, V., Ginoux, P., Komguem, L., Linné, H., López Marquez, M. Á., Matthias, V., Mattis, I., Mitev, V., Müller, D., Music, S., Nickovic, S., Pelon, J., Sauvage, L., Sobolewsky, P., Srivastava, M. K., Stohl, A., Torres, O., Vaughan, G., Wandinger, U., Wiegner, M.: Long-range transport of Saharan dust to norther Europe: The 11-16 October 2001 outbreak observed with EARLINET, J. Geophys. Res., 108, 4783, doi: 10.1029/1003JD003757, 2003

Archuleta C. M., DeMott, P. J., Kreidenweis, S. M.: Ice nucleation by surrogates for atmospheric mineral dust and mineral dust/sulfate particles at cirrus temperatures, Atmos. Chem. Phys., 5, 2617-2634, doi: 10.5194/acp-5-2617-2005, 2005

Baltensperger, U., Schwikowski, M., Jost, D. T., Nyeki, S., Gäggeler, H. W., Poulida, O.: Scavenging of atmospheric constituents in mixed phase clouds at the high-alpine site Jungfraujoch Part I: Basic concept and aerosol scavenging by clouds, Atmos. Environ., Vol. 32, No. 23, 3975-3983, 1998

Boose, Y., Welti, A., Atkinson, J., Ramelli, F., Danielczok, A., Bingemer, H. G., Plötze, M., Sierau, B., Kanji, Z. A., Lohmann, U.: Heterogeneous ice nucleation on dust particles sourced from nine deserts worldwide – Part 1: Immersion freezing, Atmos. Chem. Phys., 16, 15075-15095, doi: 10.5194/acp-16-15075-2016, 2016

Brands, M., Kamphus, M., Böttger, T., Schneider, J., Drewnick, F., Roth, A., Curtius, J. Voigt, C., Borbon, A., Beekmann, M., Bourdon, A., Perrin, T., Borrmann, S.: Characterization of a Newly Developed Aircraft-Based Laser Ablation Aerosol Mass Spectrometer (ALABAMA) and First Field Deployment in Urban Pollution Plumes over Paris During MEGAPOLI 2009, Aerosol Sci. Tech., 45:1, 46-64, doi: 10.1080/02786826.2010.517813, 2011

Brasseur, Z., Castarède, D., Thomson, E. S., Adams, M. P., Drossaart van Dusseldorp, S., Heikkilä, P., Korhonen, K., Lampilahti, J., Paramonov, M., Schneider, J., Vogel, F., Wu, Y., Abbatt, J. P. D., Atanasova, N. S., Bamford, D. H., Bertozzi, B., Boyer, M., Brus, D., Daily, M. I., Fösig, R., Gute, E., Harrison, A. D., Hietala, P., Höhler, K., Kanji, Z. A., Keskinen, J., Lacher, L., Lampimäki, M., Levula, J., Manninen, A., Nadolny, J., Peltola, M., Porter, G. C. E., Poutanen,

https://doi.org/10.5194/egusphere-2024-2797
Preprint. Discussion started: 19 September 2024
© Author(s) 2024. CC BY 4.0 License.

P., Proske, U., Schorr, T., Umo, N. S., Stenszky, J., Virtanen, A., Moisseev, D., Kulmala, M., Murray, B. J., Petäjä, T., Möhler, O., Duplissy, J.: Measurement report: Introduction to the HyICE-2018 campaign for measurements of ice-nucleating particles and instrument inter-comparison in the Hyytiälä boreal forest, Atmos. Chem. Phys., 22, 5117-5145, doi: 10.5194/acp-22-5117-2022, 2022

Bukowiecki, N., Weingartner, E., Gysel, M., Collaud Coen, M, Zieger, P., Herrmann, E., Steinbacher, M., Gäggeler H. W., Baltensperger U.: A Review of More than 20 Years of Aerosol Observation at the High-Altitude Research Station Jungfraujoch, Switzerland (3580 m asl), Aerosol Air Qual. Res., 16, 764-788, doi: 10.4209/aaqr.2015.05.0305, 2016

Burrows, S. M., McCluskey, C. S., Cornwell, G., Steinke, I., Zhang, K., Zhao, B., Zawadowicz, M., Raman, A., Kulkarni, G., China, S., Zelenyuk, A., DeMott, P. J.: Ice-Nucleating Particles That Impact Clouds and Climate: Observational and Modeling Research Needs, Rev. Geophys., 60, doi: 10.1029/2021RG000745, 2022

Cozic, J., Mertes, S., Verheggen, B., Cziczo, D. J., Gallavardin, S. J., Walter, S., Baltensperger, U., Weingartner, E.: Black carbon enrichment in atmospheric ice particle residuals observed in lower tropospheric mixed phase clouds, J. Geophys. Res., 113, D15209, doi: 10.1029/2007JD009266, 2008

Cziczo, D. J., Stetzer, O., Worringen, A., Ebert, M., Weinbruch, S., Kamphus, M., Gallavardin, S. J., Curtius, J., Borrmann, S. Froyd, K. D., Mertes, S., Möhler, O., Lohmann, U.: Inadvertent climate modification due to anthropogenic lead, Nat. Geosci., 2, 333-336, doi: 10.1038/ngeo499, 2009

Cziczo, D. J., Froyd, K. D., Hoose, C., Jensen, E. J., Diao, M., Zondlo, M. A., Smith, J. B., Twohy, C. H., Murphy, D. M.: Clarifying the Dominant Sources and Mechanisms of Cirrus Cloud Formation, Science, Vol. 340, 1320 – 1324, doi: 10.1126/science.1234145, 2013

Cziczo, D. J., Ladino, L., Boose, Y., Kanji, Z. A., Kupiszewski, P., Lance, S., Mertes, S., Wex, H.: Measurements of Ice Nucleating Particles and Ice Residuals, Meteor. Mon., 58, 1-13, doi: 10.1175/AMSMONOGRAPHS-D-16-0008.1, 2017

DeMott, P. J., Prenni, A. J., Liu, X., Kreidenweis, S. M., Petters, M. D., Twohy, C. H., Richardson, M. S., Eidhammer, T., Rogers, D. C.: Predicting global atmospheric ice nuclei distributions and their impacts on climate, P. Natl. A. Sci, 107, no. 25, 11217-11222, doi: 10.1073/pnas.0910818107, 2010

DeMott, P. J., Möhler, O., Cziczo, D., Hiranuma, N., Petters, M. D., Petters, S. S., Belosi, F., Bingemer, H. G., Brooks, S. D., Budke, C., Burkert-Kohn, M., Collier, K. N., Danielczok, A., Eppers, O., Felgitsch, L., Garimella, S., Grothe, H.,

https://doi.org/10.5194/egusphere-2024-2797
Preprint. Discussion started: 19 September 2024
© Author(s) 2024. CC BY 4.0 License.

Herenz, P., Hill, T. C. J., Höhler, K., Kanji, Z. A., Kiselev, A., Koop, T., Kristensen, T. B., Krüger, K., Kulkarni, G., Levin, E. J. T., Murray, B. J., Nicosia, A., O'Sullivan, D., Peckhaus, A., Polen, M. J., Price, H. C., Reicher, N., Rothenberg, D. A., Rudich, Y., Santachiara, G., Schiebel, T., Schrod, J., Seifreid, T. M., Stratmann, F., Sullivan, R. C., Suski, K. J., Szakáll, M., Taylor, H. P., Ullrich, R., Vergara-Temprado, J., Wagner, R., Whale, T. F., Weber, D., Welti, A., Wilson, T. W., Wolf, M. J., Zenker, J.: The Fifth International Workshop on Ice Nucleation phase 2 (FIN-02): laboratory intercomparison of ice nucleation measurements, Atmos. Meas. Tech., 11, 6231-6257, doi: 10.5194/amt-11-6231-2018, 2018

DeMott, P. J., Mirrielees, J. A., Petters, S., S., Cziczo, D. J., Petters, M. D., Bingemer, H. G., Hill, T. C. J., Froyd, K., Garimella, S., Hallar, A. G., Levin, E. J. T., McCubbin, I. B., Perring, A. E., Rapp, C. N., Schiebel, T., Schrod, J., Suski, K. J., Weber, D., Wolf, M. J., Zawadowicz, M., Zenker, J., Möhler, O., Brooks, S. D.: The Fifth International Workshop on Ice Nucleation Phase 3 (FIN-03): Field Intercomparison of Ice Nucleation Measurements, EGUsphere [preprint], doi: 10.5194/egusphere-2024-1744, 21 June 2024

Després, V. R., Huffman, J. A., Burrows, S. M., Hoose, C., Safatov A. S., Buryak G., Fröhlich-Nowoisky, J., Elbert, W., Andreae, M. O., Pöschl, U., Jaenicke, R.: Primary biological aerosol particles in the atmosphere: a review, Tellus B, 64:1, doi: 10.3402/tellusb.v64i0.15598, 2012

Ebert, M., Weinbruch, S., Hoffmann, P., Ortner, H. M.: Chemical characterization of North Sea aerosol particles, J. Aerosol Sci., Vol. 31, No. 5, 613-632, 2000

Ebert, M., Worringen, A., Benker, N., Mertes, S., Weingartner, E., Weinbruch, S.: Chemical composition and mixing-state of ice residuals sampled within mixed phase clouds, Atmos. Chem. Phys., 11, 2805-2816, doi: 10.5194/acp-11-2805-2011, 2011

Eriksen Hammer, S., Mertes, S., Schneider, J., Ebert, M., Kandler, K., Weinbruch, S.: Composition of ice particle residuals in mixed-phase clouds at Jungfraujoch (Switzerland): enrichment and depletion of particle groups relative to total aerosol, Atmos. Chem. Phys., 18, 1387-1403, doi: 10.5194/acp-18-13987-2018, 2018

Eriksen Hammer, S., Ebert, M., Weinbruch, S.: Comparison of operator- and computer-controlled scanning electron microscopy of particles from different atmospheric aerosol types, Anal. Bioanal. Chem., 411:1633-1645, doi: 10.1007/s00216-019-01614-7, 2019

https://doi.org/10.5194/egusphere-2024-2797
Preprint. Discussion started: 19 September 2024
© Author(s) 2024. CC BY 4.0 License.

He, C., Yin, Y., Huang, Y., Kuang, X., Cui, Y., Chen, K., Jiang, H., Kiselev, A., Möhler, O., Schrod, J.: The Vertical Distribution of Ice-Nucleating Particles over the North China Plain: A Case of Cold Front Passage, Remote Sens., 15, 4989, doi: 10.3390/rs15204989, 2023

Herrmann, E., Weingartner, E., Henne, S., Vuilleumier, L., Bukowiecki, N., Steinbacher, M., Conen, F., Collaud Coen, M., Hammer, E., Jurányi, Z., Baltensperger, U., Gysel, M.: Analysis of long-term aerosol size distribution data from Jungfraujoch with emphasis on free tropospheric conditions, cloud influence, and air mass transport, J. Geophys. Res.-Atmos., 9459 – 9480, doi: 10.1002/201JD023660, 2015

Hiranuma, N., Augustin-Bauditz, S., Bingemer, H., Budke, C., Curtius, J., Danielczok, A., Diehl, K., Dreischmeier, K., Ebert, M., Frank, F., Hoffmann, N., Kandler, K., Kiselev, A., Koop, T., Leisner, T., Möhler, O., Nillius, B., Peckhaus, A., Rose, D., Weinbruch, S., Wex, H., Boose, Y., DeMott, P. J., Hader, J. D., Hill, T. C. J., Kanji, Z. A., Kulkarni, G., Levin, E. J. T., McCluskey, C. S., Murakami, M., Murray, B. J., Niedermeier, D., Petters, M. D., O'Sullivan D., Saito, A., Schill, G. P., Tajiri, T., Tolbert, M. A., Welti, A., Whale, T. F., Wright T. P., Yamashita, K.: A comprehensive laboratory study on the immersion freezing behavior of illite NX particles: a comparison of 17 ice nucleation measurement techniques, Atmos. Chem. Phys., 15, 2489-2518, doi: 10.5194/acp-15-2489-2015, 2015

Hiranuma, N., Adachi, K., Bell, D. M., Belosi, F., Beydoun, H., Bhaduri, B., Bingemer, H., Budke, C., Clemen, H.-C., Conen, F., Cory, K. M., Curtius, J., DeMott, P. J., Eppers, O., Grawe, S., Hartmann, S., Hoffmann, N., Höhler, K., Jantsch, E., Kiselev, A., Koop, T., Kulkarni, G., Mayer, A., Murakami, M., Murray, B. J., Nicosia, A., Petters, M. D., Piazza, M., Polen, M., Reicher, N., Rudich, Y., Saito, A., Santachiara, G., Schiebel, T., SChill, G. P., Schneider, J., Segev, L., Stopelli, E:, Sullivan, R. C., Suski, K., Szakáll, M., Tajiri, Z., Taylor, H., Tobo, Y., Ullrich, R., Weber, D., Wex, H., Whale, T. F., Whiteside, C. L., Yamashita, K., Zelenyuk, A., Möhler, O.: A comprehensive characterization of ice nucleation by three different types of cellulose particles immersed in water, Atmos. Chem. Phys., 19, 4823-4849, doi: 10.5194/acp-19-4823-2019, 2019

Hoose, C. and Möhler, O.: Heterogeneous ice nucleation on atmospheric aerosols: a review of results from laboratory experiments, Atmos. Chem. Phys., 12, 9817-9854, doi: 10.5194/acp-12-9817-2012, 2012

Jing, X., Yang, J., Li, T., Hu, J., He, C., Yin, Y., DeMott, P. J., Wang, Z., Jiang, H., Chen, K.: Pre-Activation of Ice Nucleating Particles in Deposition Nucleation Mode: Evidence from Measurement Using a Static Vacuum Water Vapor Diffusion Chamber in Xinjiang, China, Geophys. Res. Lett., 49, e2022GL099468, doi: 10.1029/2022GL099468, 2022

https://doi.org/10.5194/egusphere-2024-2797
Preprint. Discussion started: 19 September 2024
© Author(s) 2024. CC BY 4.0 License.

Kamphus, M., Ettner-Mahl, M., Klimach, T., Drewnick, F., Keller, L., Cziczo, D. J., Mertes, S., Borrmann, S., Curtius, J.: Chemical composition of ambient aerosol, ice residues and cloud droplet residues in mixed-phase clouds: single particle analysis during the Cloud and Aerosol Characterization Experiment (CLACE 6), Atmos. Chem. Phys., 10, 8077-8095, doi: 10.5194/acp-10-8077-2010, 2010

Kandler, K., Benker, N., Bundke, U., Cuevas, E., Ebert, M., Knippertz, P., Rodríguez, E., Schütz, L., Weinbruch, S.: Chemical composition and complex refractive index of Saharan Mineral Dust at Izaña, Tenerife (Spain) derived by electron microscopy, Atmos. Environ. 41, 8058-8074, doi: 10.1016/j.atmosenv.2007.06.047, 2007

Kanji, Z. A., Florea, O., Abbatt, J. P. D.: Ice formation via deposition nucleation on mineral dust and organics: dependence of onset relative humidity on total particulate surface area, Environ. Res. Lett., 3, 025004, doi: 10.1088/1748-9326/3/2/025004, 2008

Kanji, Z. A., Ladino, L. A., Wex, H., Boose, Y., Burkert-Kohn, M., Cziczo, D. J., Krämer, M.: Overview of Ice Nucleating Particles, Meteor. Mon., Vol. 58, doi: 10.1175/AMSMONOGRAPHS-D-16-0006.1, 2017

Kiselev, A., Bachmann, F., Pedevilla, P., Cox, S. J., Michaelides, A., Gerthsen, D., Leisner, T.: Active sites in heterogeneous ice nucleation – the example of K-rich feldspars, Science, 10, doi: 10.1126/science.aai8034, 2016

Klein, H., Haunold, W., Bundke, U., Nillius, B., Wetter, T., Schallenberg, S., Bingemer, H.: A new method for sampling of atmospheric ice nuclei with subsequent analysis in a static diffusion chamber, Atmos. Res., 96, 218-224, doi: 10.1016/j.atmores.2009.08.002, 2010

Kupiszewski, P., Weingartner, E., Vochezer, P., Schnaiter, M., Bigi, A., Gysel, M., Rosati, B., Toprak, E., Mertes, S., Baltensperger, U.: The Ice Selective Inlet. A novel technique for exclusive extraction of pristine ice crystals in mixed-phase clouds, Atmos. Meas. Tech., 8, 3087-3106, doi: 10.5194/amt-8-3087-2015, 2015

Kupiszewski, P., Zanatta, M., Mertes, S., Vochezer, P., Lloyd, G., Schneider, J., Schenk, L., Schnaiter, M., Baltensperger, U., Weingartner, E., Gysel, M.: Ice residual properties in mixed-phase clouds at the high-alpine Jungfraujoch site, J. Geophys. Res.-Atmos, 121, 12343-12362, doi: 10.1002/2016JD024894, 2016

Lacher, L., Clemen H.-C., Shen, X., Mertes, S., Gysel-Beer, M., Moallemi, A., Steinbacher, M., Henne, S., Saathoff, H., Möhler, O., Höhler, K., Schiebel, T., Weber, D., Schrod, J., Schneider, J., Kanji, Z. A.: Sources and nature of ice-

https://doi.org/10.5194/egusphere-2024-2797
Preprint. Discussion started: 19 September 2024
© Author(s) 2024. CC BY 4.0 License.

nucleating particles in the free troposphere at Jungfraujoch in winter 2017, Atmos. Chem. Phys., 21, 16925-16953, doi: 10.5194/acp-21-16925-2021, 2021

Lacher, L., Adams, M. P., Barry, K., Bertozzi, B., Bingemer, H., Boffo, C., Bras, Y., Büttner, N., Castarede, D., Cziczo, D. J., DeMott, P. J., Fösig, R., Goodell, M., Höhler, K., Hill, T. C. J., Jentzsch, C., Ladino, L. A., Levin, E. J. T., Mertes, S., Möhler, O., Moore, K. A., Murray, B. J., Nadolny, J., Pfeuffer, T., Picard, D., Ramírez-Romero, C., Ribeiro, M., Richter, S., Schrod, J., Sellegri, K., Stratmann, F., Swanson, B. E., Thomson E. S., Wex, H., Wolf, M. J., Freney, E.: The Puy de Dôme ICe Nucleation Intercomparison Campaign (PICNIC): comparison between online and offline methods in ambient air, Atmos. Chem. Phys., 24, 2651-2678, doi: 10.5194/ACP-24-2651-2024, 2024

Lohmann, U., Lüönd, F., Mahrt, F.: An introduction to clouds, p. 229, Cambridge University Press, Cambridge, U.K., 381 pp., 2016

Mertes, S., Verheggen, B., Walter, S., Connolly, P., Ebert, M., Schneider, J., Bower, K. N., Cozic, J., Weinbruch, S., Baltensperger, U., Weingartner, E.: Counterflow Virtual Impactor Based Collection of Small Ice Particles in Mixed-Phase Clouds for the Physico-Chemical Characterization of Tropospheric Ice Nuclei: Sampler Description and First Case Study, Aerosol Sci. Tech., 41, 848-864, doi: 10.1080/02786820701501881, 2007

Murray, B. J. and Liu, X.: Ice-nucleating particles and their effects on clouds and radiation, in: Aerosols and Climate, edited by Carslaw, K. S., Elsevier, 619-649, doi:10.1016/B978-0-12-819766-0.00014-6, 2022

Nyeki, S., Li, F., Weingartner, E., Streit, N., Colbeck, I., Gäggeler, H. W., Baltensperger, U.: The background aerosol size distribution in the free troposphere: An analysis of the annual cycle at a high-alpine site, J. Geophys. Res., Vol. 103, D24, 31749-31761, doi: 10.1029/1998JD200029, 1998

Okada, K. and Kai, K.: Atmospheric mineral particles collected at Qira in the Taklamakan Desert, China, Atmos. Environ. 38, 6927-6935, doi: 10.1016/j.atmosenv.2004.03.078, 2004

O'Sullivan, D., Murray, B. J., Malkin, T. L., Whale, T. F., Umo, N. S., Atkinson, J. D., Price, H. C., Baustian, K. J., Browse, J., Webb, M. E.: Ice nucleation by fertile soil dusts: relative importance of mineral and biogenic components, Atmos. Chem. Phys., 14, 1853-1867, doi: 10.5194/acp-14-1853-2014, 2014

Perry, K. D., Cahill, T. A., Eldred, R. A., Dutcher, D. D.: Long-range transport of North African dust to the eastern United States, J. Geophys. Res., 102, 11,225-11,238, doi: 10.1029/97JD00260, 1997

https://doi.org/10.5194/egusphere-2024-2797
Preprint. Discussion started: 19 September 2024
© Author(s) 2024. CC BY 4.0 License.

Petters, M. D. and Wright, T. P.: Revisiting ice nucleation from precipitation samples, Geophys. Res. Lett., 42, 8758-8766, doi: 10.1002/2015GL065733, 2015

Pratt, K. A., DeMott, P. J., French, J. R., Wang, Z., Westphal, D. L., Heymsfield, A. J., Twohy, C. H., Prenni, A. J., Prather, K. A.: In situ detection of biological particles in cloud ice-crystals, Nat. Geosci., Vol. 2, 398 – 401, doi: 10.1038/NGEO521, 2009

Prenni, A. J., Petters, M. D., Kreidenweis, S. M., Heald, C. L., Martin, S. T., Artaxo, P., Garland, R. M., Wolly, A. G., Pöschl, U.: Relative roles of biogenic emissions and Saharan dust and ice nuclei in the Amazon basin, Nat. Geosci., Vol. 2, 402-405, doi: 10.1038/NGEO517, 2009

Pummer, B. G., Bauer, H., Bernardi, J., Bleicher, S., Grothe, H.: Suspendable macromolecules are responsible for ice nucleation activity of birch and conifer pollen, Atmos. Chem. Phys., 12, 2541-2550, doi: 10.5194/acp-12-2541-2012, 2012

Rogers, D. C.: Development of a Continuous Flow Thermal Gradient Diffusion Chamber for Ice Nucleation Studies, Atmos. Res., 22, 149-181, 1988

Schenk, L. P., Mertes, S., Kästner, U., Frank, F., Nillius, B., Bundke, U., Rose, D., Schmidt, S., Schneider, J., Worringen, A., Kandler, K., Bukowiecki, N., Ebert, M., Curtius, J., Stratmann, F.: Characterization and first results of an ice nucleating particle measurement system based on counterflow virtual impactor technique, Atmos. Meas. Tech. Discuss., 7, 10585-10617, doi: 10.5194/amtd-7-10585-2014, 2014

Schepanski, K.: Transport of Mineral Dust and Its Impact on Climate, Geosiences 2018, 8, 151, doi: 10.3390/geoscience8050151, 2018

Scheuvens, D. and Kandler, K.: On Composition, Morphology, and Size Distribution of Airborne Mineral Dust, in: Mineral Dust, edited by Knippertz, P. and Stuut, J.-B. W., Springer, Dordrecht, doi: 10.1007/978-94-017-8978-3_2, 2014

Schmidt, S., Schneider, J., Klimach, T., Mertes, S., Schenk, L. P., Kupiszewski, P., Curtius, J., Borrmann, S.: Online single particle analysis of ice particle residuals from mountain-top mixed-phase clouds using laboratory derived particle type assignment, Atmos. Chem. Phys., 17, 575-594, doi: 10.5194/acp-17-575-2017, 2017

https://doi.org/10.5194/egusphere-2024-2797
Preprint. Discussion started: 19 September 2024
© Author(s) 2024. CC BY 4.0 License.

Schneider, C. A., Rasband, W. S., Eliceiri, K. W., NIH Image to ImageJ: 25 years of image analysis, Nat. Methods, 9(7), 671-675, doi: 10.1038/nmeth.2089, 2012

Schrod, J., Danielczok, A., Weber, D., Ebert, M., Thomson E. S., Bingemer H. G.: Re-evaluating the Frankfurt isothermal static diffusion chamber for ice nucleation, Atmos. Meas. Tech., 9, 1313-1324, doi: 10.5194/amt-9-1313-2016, 2016

Schrod, J., Weber, D., Drücke, J., Keleshis, C., Pikridas, M., Ebert, M., Cvetkovic, B., Nickovic, S., Marinou, E., Baars, H., Ansmann, A., Vrekoussis, M., Mihalopoulos, N., Sciare, J., Curtius, J., Bingemer, H. G.: Ice nucleating particles over the Eastern Mediterranean measured by unmanned aircraft systems, Atmos. Chem. Phys., 17, 4817-4835, doi: 10.5194/acp-17-4817-2017, 2017

Schrod, J., Kleinhenz, D., Hörhold, M., Erhardt, T., Richter, S., Wilhelms F., Fischer, H., Ebert, M., Twarloh, B., Della Lunga, D., Jensen, C. M., Curtius, J., Bingemer, H. G.: Ice-nucleating particle concentrations of the past: insights from a 600-year-old Greenland ice core, Atmos. Chem. Phys., 20, 12459-12482, doi: 10.2194/acp-20-12459-2020, 2020a

Schrod, J., Thomson E. S., Weber, D., Kossmann, J., Pöhlker, C., Saturno J., Ditas, F., Artaxo, P., Clouard, V., Saurel, J.-M., Ebert, M., Curtius, J., Bingemer, H. G.: Long-term deposition and condensation ice-nucleating particle measurements from four stations across the globe, Atmos. Chem. Phys., 20, 15983 – 16006, doi: 10.5194/acp-20-15983-2020, 2020b

Schwarzenboeck, A., Heintzenberg, J., Mertes, S.: Incorporation of aerosol particles between 25 and 850 nm into cloud elements: measurments with a new complementary sampling system, Atmos. Res., 25, 241-260, doi: 10.1016/S0169-8059(99)00034-4, 2000

Sorensen, C. M., Feke, G. D.: The Morphology of Macroscopic Soot, Aerosol Sci. Tech., 25, 328-337, doi:10.1080/02786829608965399, 1996

Thomson, D. S., Schein, M. E., Murphy, D. M.: Particle Analysis by Laser Mass Spectrometry WB-57F Instrument Overview, Aerosol Sci. Tech., 33:153-169, doi: 10.1080/027868200410903, 2000

Vali, G., DeMott, P. J., Möhler, O., Whale, T. F.: Technical Note: A proposal for ice nucleation terminology, Atmos. Chem. Phys., 15, 10263 – 10270, doi: 10.5194/acp-15-10263-2015, 2015

https://doi.org/10.5194/egusphere-2024-2797
Preprint. Discussion started: 19 September 2024
© Author(s) 2024. CC BY 4.0 License.

Weber, D.: Eisnukleation von Aerosolen: Laborexperimente und Messungen im Feld, Ph.D. thesis, Goethe Universität Frankfurt, Germany, 2019

Wex, H., Huang, L., Zhang, W., Hung, H., Traversi, R., Becagli, S., Sheesley, R. J., Moffett, C. E., Barrett, T. E., Bossi, R., Skov, H., Hünerbein, A., Lubitz, J., Löffler, M., Linke, O., Hartmann, M., Herenz, P., Stratmann, F.: Annual variability of ice-nucleating particle concentrations at different Arctic locations, Atmos. Chem. Phys., 19,5293-5311, doi: 10.5194/acp-19-5293-2019, 2019

Whalley, W. B. and Krinsley, D. H.: A scanning electron microscope study of surface textures of quartz grains from glacial environments, Sedimentology, 21, 87-105, doi:10.1111/j.1365-3091.1974.tb01783.x, 1974

Worringen, A., Kandler, K., Benker, N., Dirsch, T., Mertes, S., Schenk, L., Kästner, U., Frank, F., Nillius, B., Bundke, U., Rose, D., Curtius, J., Kupiszewski, P., Weingartner, E., Vochezer, P., Schneider, J., Schmidt, S. Weinbruch, S., Ebert, M.: Single-particle characterization of ice-nucleating particles and ice particle residuals sampled by three different techniques, Atmos. Chem. Phys., 15, 4161-4178, doi: 10.5194/acp-15-4161-2015, 2015